STUDY OF WOOD-FRAME BUILDING RECORDS
FROM THE PARKFIELD AND SAN SIMEON EARTHQUAKES

Daniel Sutoyo and John Hall

Department of Civil Engineering
California Institute of Technology, Pasadena

Abstract

In order to develop seismic codes that can effectively mitigate damage to wood-frame construction under seismic activity, the dynamic characteristics of wood-frame buildings must be well understood. Toward this end, this data interpretation project focuses on the dynamic behavior of low-rise wooden shearwall buildings under large seismic motions. The procedure includes determining the modal parameters and extracting hysteretic characteristics from the available records.

Overview

Low-rise wood-frame buildings are the predominant wood-frame construction in North America. In California, 99% of all residences are constructed of wood (Camelo 2002). Due to the ubiquitous nature of wood-frame construction, it is surprising that wood-frame building behavior is not fully understood. Progress is being made though as this topic has attracted a lot of government and research attention in recent years, primarily because of huge economic losses in '94 Northridge earthquake. Advancement in wood-frame research has been made through the collaboration of Federal Emergency Management Agency (FEMA) and the Consortium of Universities of Research in Earthquake Engineering (CUREE). The ultimate goal of such work is to make the basis of building codes more rational. The project covered five main areas: testing and analysis, field investigations, building codes and standards, economic aspects and education and outreach (Camelo 2002).

As part of the CUREE project, Camelo and Beck performed system identification with the computed program MODE-ID (Beck 1987) on several wooden buildings California Strong Motion Instrumentation Program (CSMIP) sites. The results show that there is clear amplitude dependence; fundamental frequencies were lowest and damping estimates were highest in the time frame of the strongest seismic activity (Camelo 2003). An important feature from the analysis was the high damping estimates. The values ranged from 15-20%, which are several times more than that of steel or concrete structures.

The current project extends the work of Camelo (2003) to two buildings at higher shaking levels. Since the estimated damping values include energy dissipated by hysteretic action, the current project also seeks to extract hysteretic characteristics of these buildings. The project has six main objectives:

1) Apply different system identification methods to obtain modal estimates. Specifically, observe if various methods conclude on high damping values for wood-frame construction. Investigate methods that include but are not limited to: SDOF time domain methods, random decrement method, frequency curve fitting methods, and Hilbert and Wavelet Transforms.

2) Using the most appropriate system identification technique, perform detailed system identification studies on two structures, Parkfield school and Templeton hospital building, for recently obtained earthquake records. The focus will be on natural frequency and damping as a function of response amplitude.

3) Extract hysteretic parameters of walls and diaphragms from the recorded time histories.

4) Perform system identification studies on components of buildings, such as diaphragms, to determine their dynamic characteristics.

5) Create numerical models to simulate the measured responses. Models will be used to confirm the estimates of various system identification methods, validate the hysteresis extraction procedures and validate the component identification process. A particular interest will be the large damping values.

6) Interpret all of the results for the benefit of code development.

Buildings and Records

Parkfield school and Templeton hospital buildings are chosen as test subjects for analysis. Previous studies have successfully been conducted at these locations, and there is a plethora of records and documentation from past studies contained within the CSMIP database. The databases contain several records of these buildings at different amplitudes of shaking, including the record for the largest peak structural acceleration in a wood-frame building at 128% g.

Parkfield School

Parkfield - 1-story School Bldg
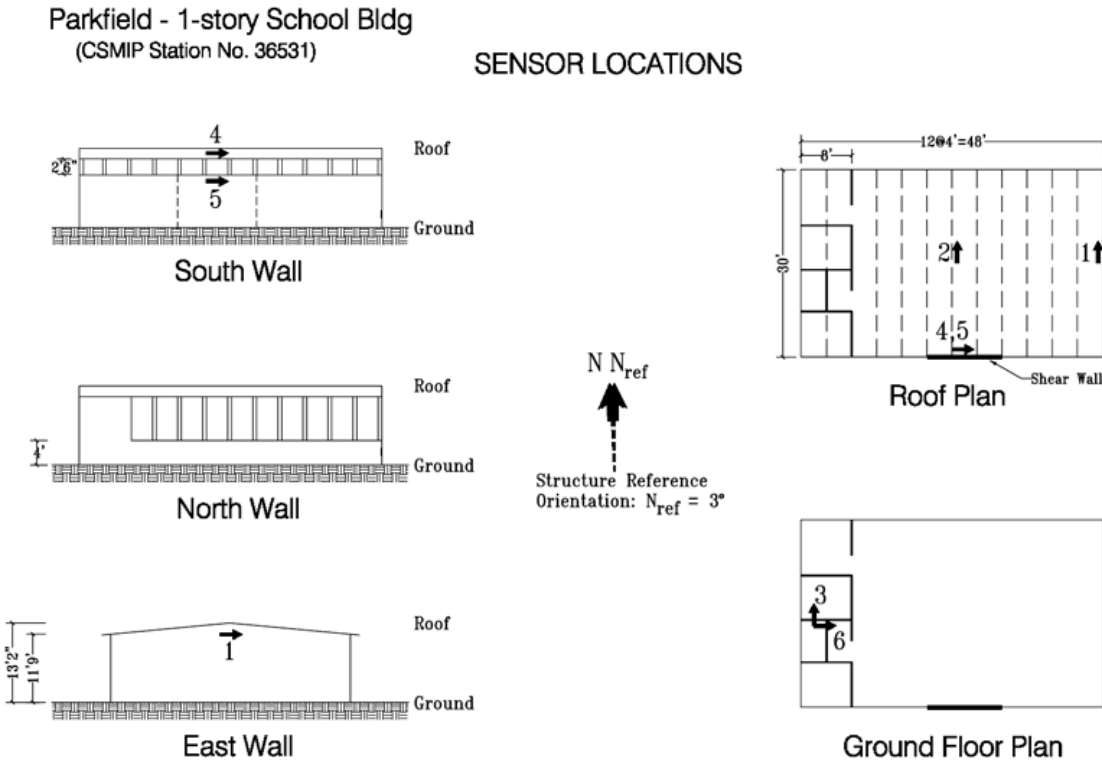(CSMIP Station No. 36531)

SENSOR LOCATIONS

Figure 1: A schematic of Parkfield school building displaying the locations of all six sensors.

The Parkfield school building, built in 1949, is a rectangular wood-frame building with dimensions of 48' by 30' (Figure 1). There are a total of six accelerometer channels on the building. Channels 3 and 6 are the ground reference and taken as the excitation when using MODE-ID. Two channels are in the N-S (transverse) direction and two are in the E-W (longitudinal) direction. Figure 2 displays the acceleration time histories recorded during the 2004 Parkfield earthquake.
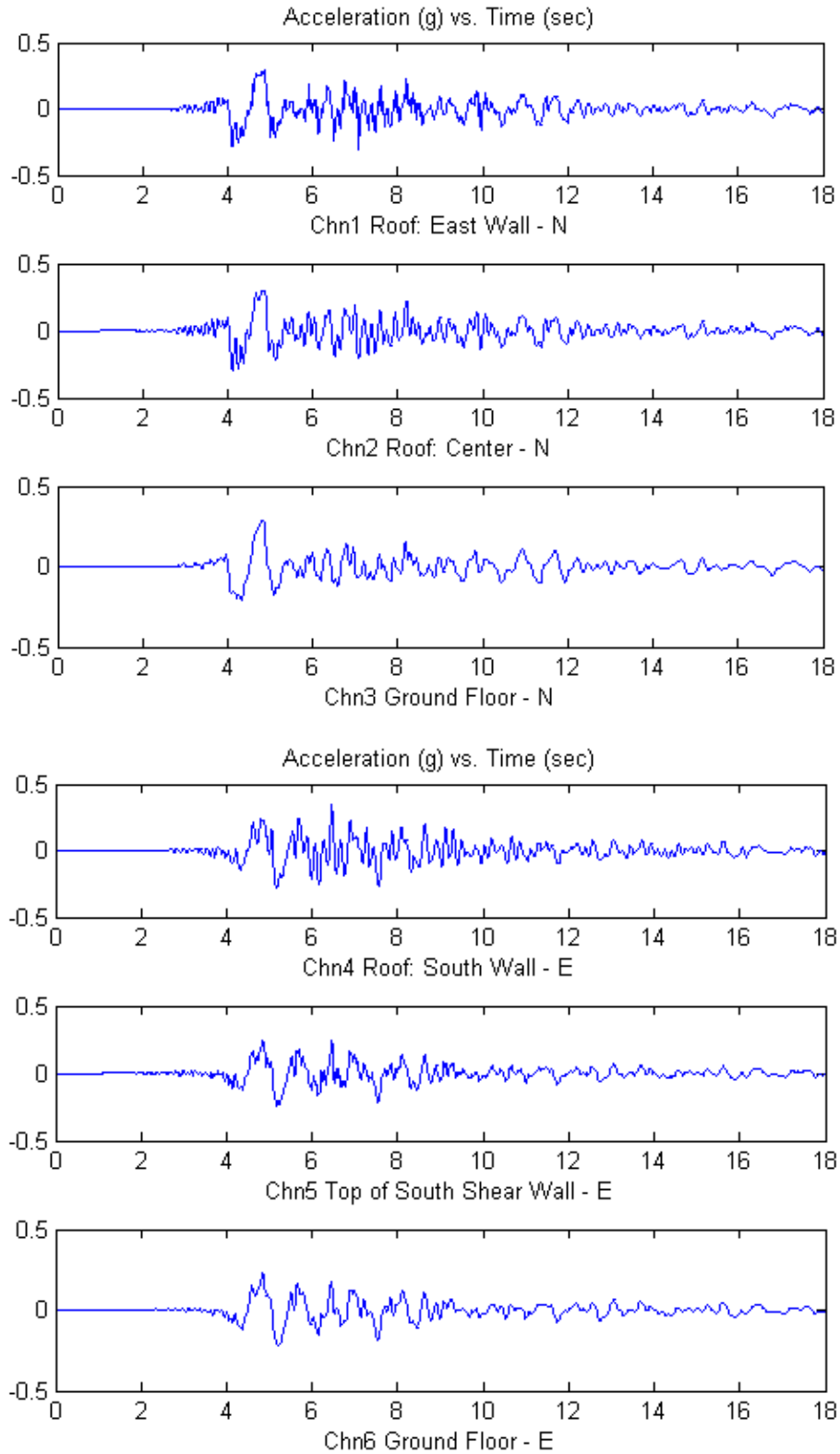
Figure 2: Acceleration time histories that were recorded from the Parkfield school building during the 2004 Parkfield earthquake.

Templeton Hospital

The Templeton hospital building, built in the 1970s, has an irregular shaped building plan spanning the dimensions of 336' by 277' (Figure 3). There are a total of nine accelerometer channels on the building. Channels 1 (vertical), 2 (E-W) and 3 (N-S) are the ground reference sensors. There are three channels for each N-S and E-W direction. Figure 4 displays the acceleration time histories recorded during the 2003 San Simeon earthquake.
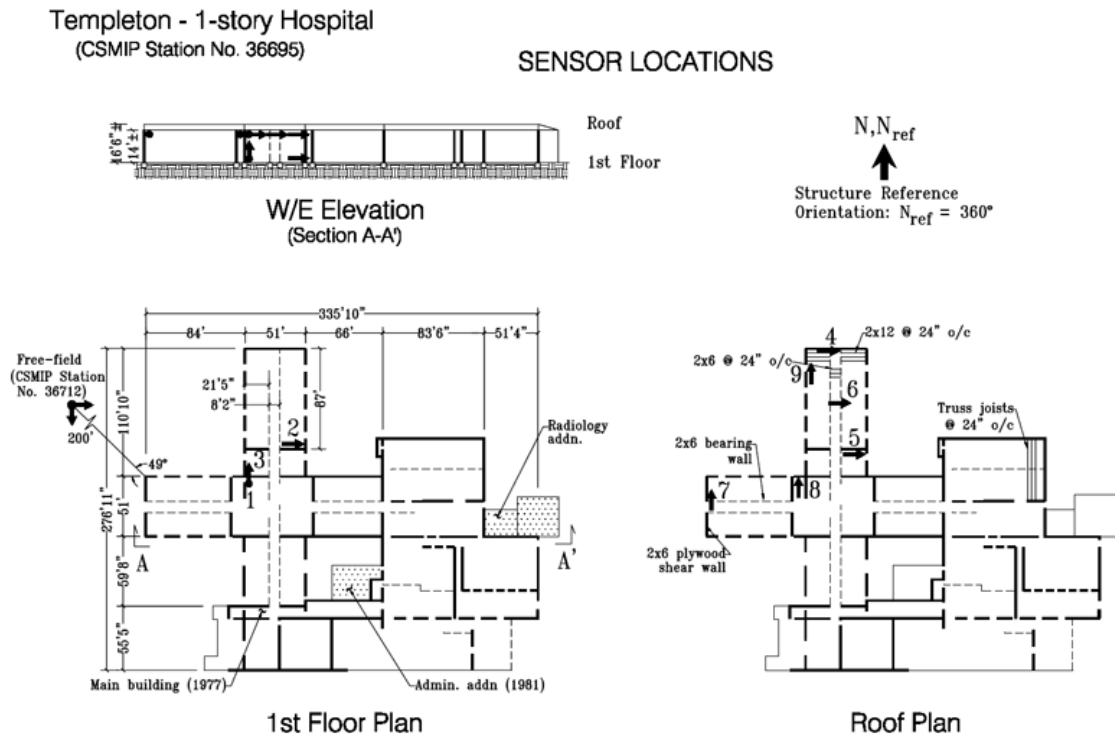
Figure 3: A schematic of Templeton hospital building displaying the locations of all nine sensors.
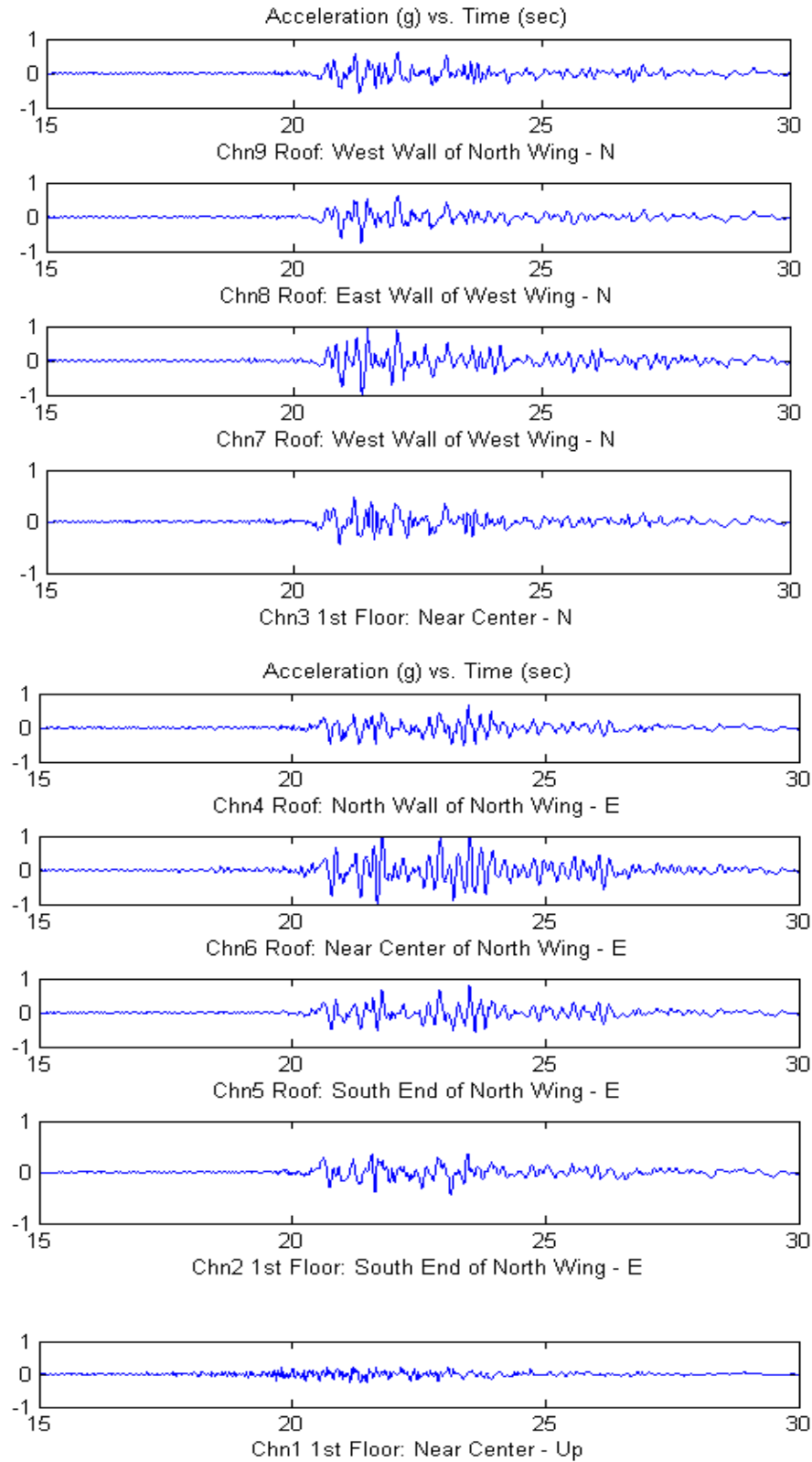
Figure 4: Acceleration time histories that were recorded from the Templeton hospital building during the 2003 San Simeon earthquake.

System Identification

Various system identification schemes were explored, but MODE-ID is selected for its robustness. MODE-ID utilizes modal identification and a modal minimization routine (Beck and Beck 1985). Modal identification estimates modal parameters of a linear dynamic model from the responses of a structure. This application of system identification can be performed in the time domain without the need to develop a structural model by constructing mass, stiffness and damping matrices (Beck, 1978).

Without discussing all the other methods in detail, most of them are ad-hoc, requiring special conditions not met in practice with real seismic response records. Assumptions can be made to improve the results of other methods, but this process requires specific tailoring of the records. However, this is not to say MODE-ID is the only method that is suitable for analyzing real seismic records. Other estimation methods like Bayseian approaches and particle filtering could be suitable as well (Ching, et al.2004). Furthermore a frequency domain MODE-ID can be employed through Parseval's Inequality (Werner 1987).

MODE-ID can handle multiple inputs in order to find the modal parameters from seismic motions recorded from a structure. Inputs for MODE-ID include the ground excitation records, measured structural response histories and initial modal estimates. The modal parameters estimated for each mode are the frequency, damping factor, normalized modeshape, participation factors and initial displacement and velocity. MODE-ID has been extensively applied to earthquake and other dynamic data. In short MODE-ID is based on a nonlinear least-squares output-error method. The measure of fit between the recorded and calculated response is optimized by a modal minimization algorithm (Beck and Beck 1985).

To minimize the measure-of-fit, the program performs a series of sweeps in which optimization is performed one mode at a time. Optimization within each mode is by the method of steepest descent with respect to the modal frequency and damping (Beck and Jennings 1980). Additional information and detailed mathematical background can be found in the MODE-ID user guide and in EERL Report 85-06. Both are listed in the reference section.

Results

Parkfield School

The Parkfield school building is only one story tall. It is expected that the dominant response will largely consist of the fundamental N-S, E-W and torsional modes. The frequency, damping and modeshape estimates are presented in Table 1 and Figure 5. In addition to the 2004 Parkfield earthquake, records from two smaller earthquakes in 1993 and 1994 are considered in order to provide a range of response amplitudes. Note from Figure 5 that the modes are coupled and so are not purely N-S, E-W and torsional.

Table 1.   Parkfield school building frequency and damping estimates calculated from MODE-ID. The peak structural acceleration is provided for each earthquake

Earthquake	Frequency (Hz) E-W	Damping Ratio (%) E-W	Frequency (Hz) N-S	Damping Ratio (%) N-S	Frequency (Hz) T	Damping Ratio (%) T
4.2 M 0.123 g 04/04/1993	7.3	12.3	8.6	14.5	9.8	11.3
4.7 M 0.201 g 12/20/1994	6.5	10.7	8.2	14.0	19.2	11.1
6.0 M 0.30 g 09/28/2004	5.26	12.9	6.01	12.9	13.1	8.9

The 1993 and 1994 earthquakes have been reanalyzed and compared to the results of Camelo and Beck in CUREE Publication No. W-11. The values are found to be consistent. Since the magnitudes of the earthquake in 1993 and 1994 are similar, the reported modal frequency and damping estimates are comparable with the exception of the damping ratios of the torsional mode. A reason for this difference is not evident. With the addition of the records from 2004, amplitude dependence can be observed. The larger response amplitudes are accompanied by lower frequencies and higher damping values.

The analysis done on full-duration records displays high damping estimates as have been noted in previous studies. Damping is inherently difficult to estimate accurately with any method (Beck and Beck 1985). The credibility of a 20% damping ratio in wood-frame buildings needs to be investigated since steel or concrete buildings generally have values of 3 to 5%. For MODE-ID, a linear viscous damping is assumed. The meaning of a linear damping value that is fit under conditions of nonlinear response is currently under study.
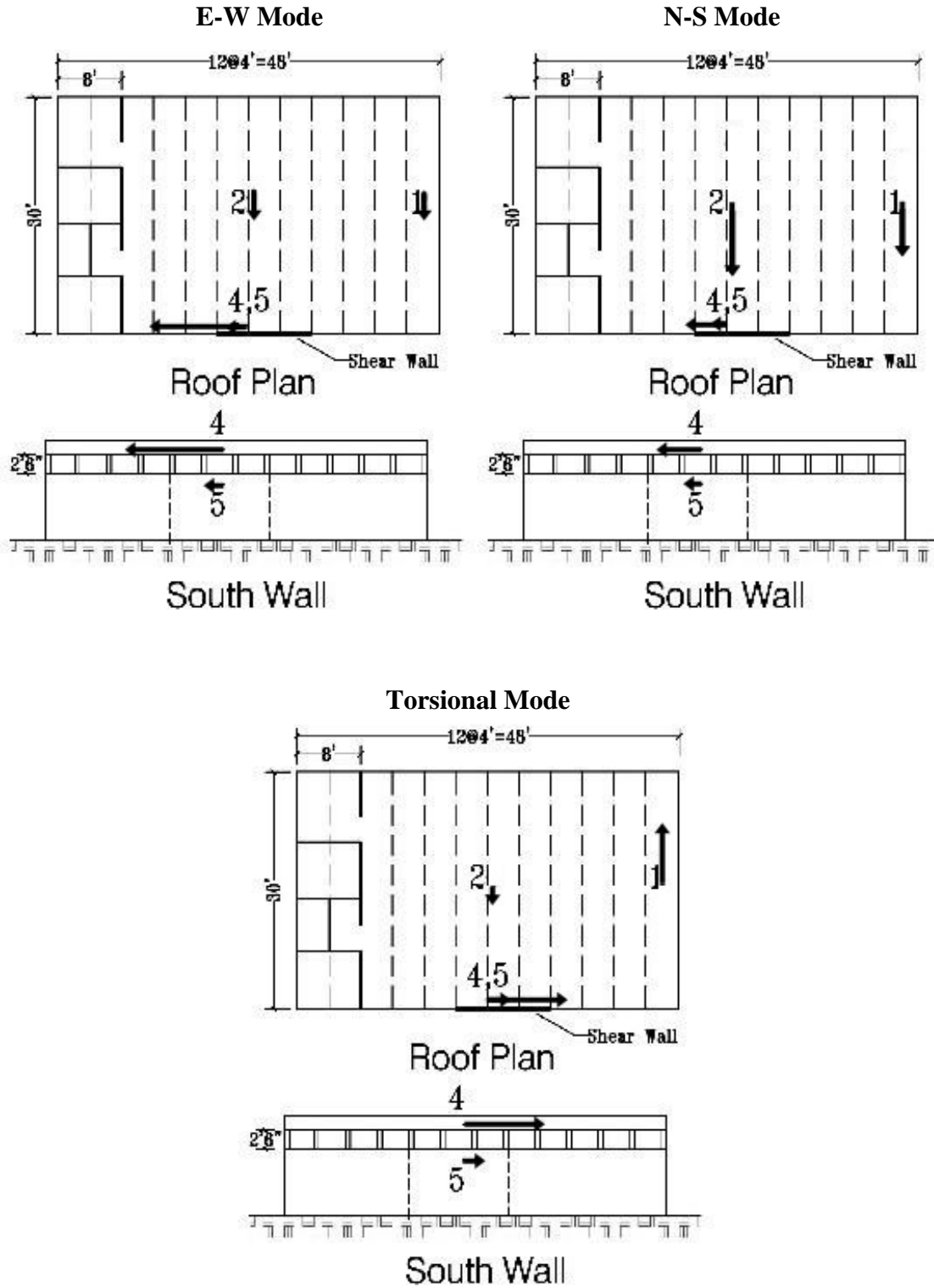
E-W Mode   **N-S Mode**

Torsional Mode

**Figure 5:   First three modeshapes of the Parkfield school building
generated from the 2004 Parkfield earthquake**

Another observation that can be inferred from Table 1 is that the damping estimates in the N-S are generally greater than those of the E-W modes. This may be related to the fact that the north and south walls have less shear wall contribution due to a substantial area designated for windows, as shown in Figure 6.
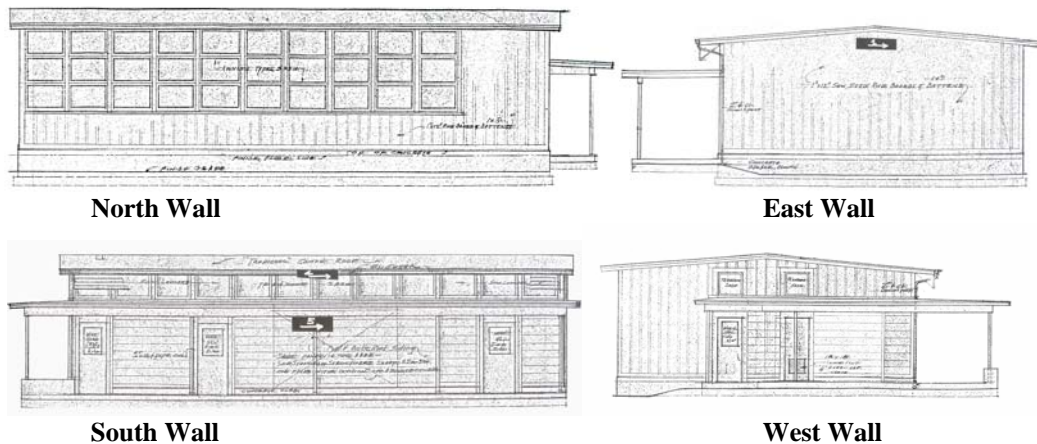

North Wall   **East Wall**

South Wall   **West Wall**

Figure 6. Elevation views of the Parkfield school building

A windowing analysis is also performed on the 2004 Parkfield records through MODE-ID. Results are presented in Figure 7 (frequencies) and Figure 8 (damping). A two-second window with 50 % overlap was chosen because it is the smallest window that results in consistent convergence. Windowing reveals the change in modal frequency and damping during the earthquake.

From Figure 7 it is apparent that the building did reach nonlinear motions as each fundamental frequency changed during the course of the response. Following the locus of the estimated fundamental frequencies of the building, the initial frequencies are around the 7.5 Hz range when the initial motion was recorded. The building's frequencies decrease as the magnitude of the ground response increases, reaching significantly lower values during the time of the strongest ground shaking at around 5 seconds (Figure 2). As the ground motion subsides, the building's frequencies revert to the initial frequencies. This probably indicates the building sustained no significant damage.

The window analysis on damping estimates (Figure 8) shows that damping fluctuates greatly throughout the earthquake shaking. Another observation is that even at lower ground motions, the damping ratio still display values of 12-20%, which are high relative to steel and concrete buildings. As mentioned previously, the issue of high damping values is currently under study.
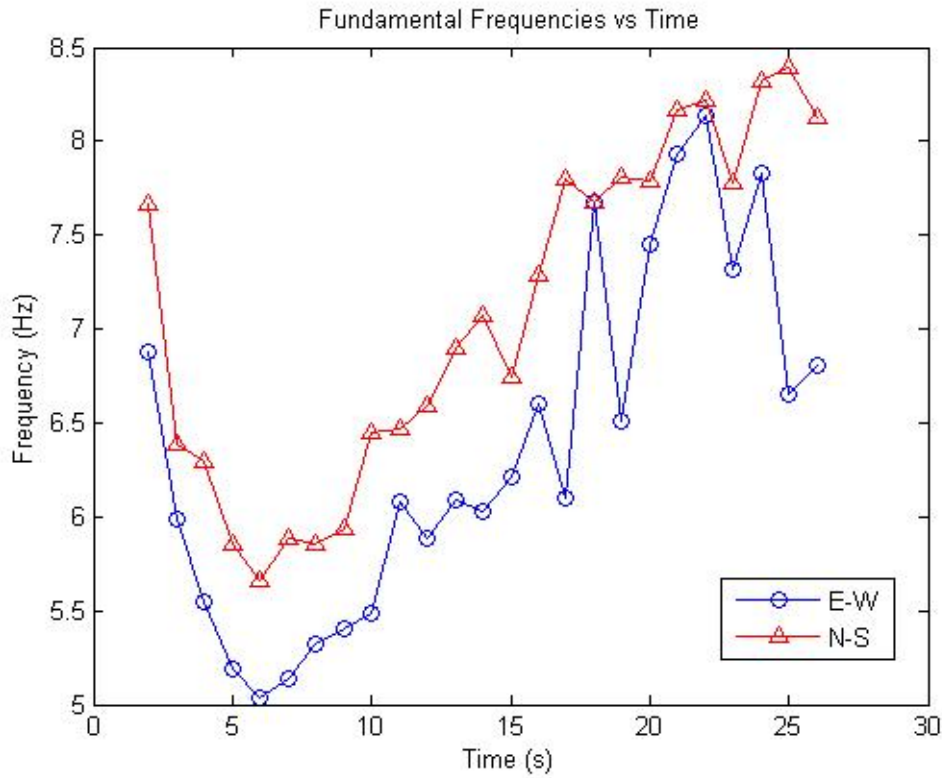
Figure 7: **Amplitude dependence of the E-W and N-S mode frequency estimates for Parkfield School building. The window analysis is performed on the 2004 Parkfield earthquake.**
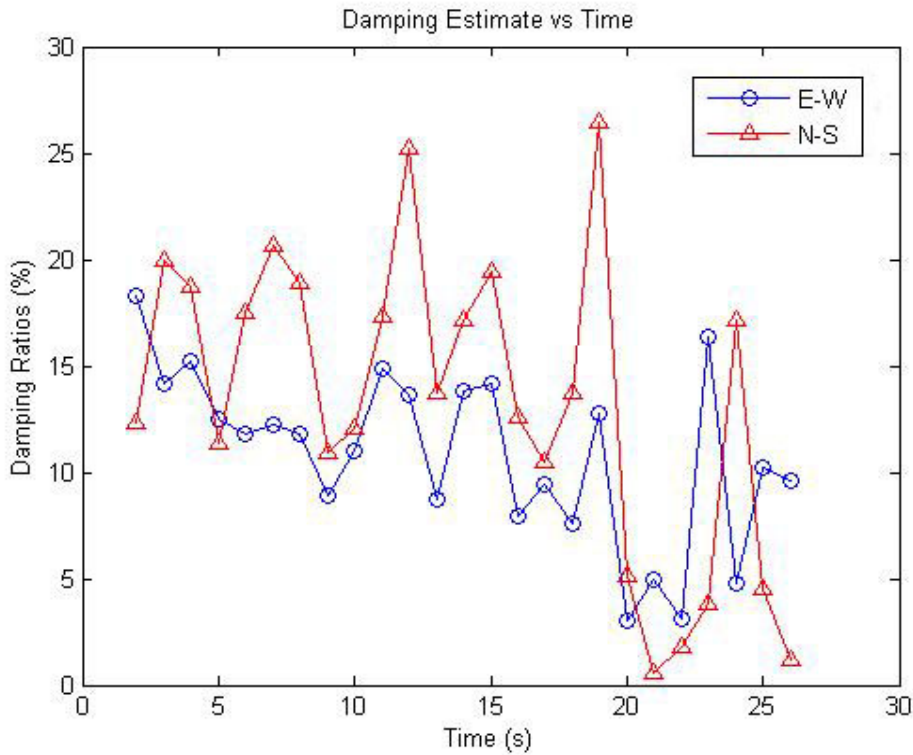

Figure 8. Amplitude dependence of the E-W and N-S mode damping estimates for Parkfield School building. The window analysis is performed on the 2004 Parkfield earthquake.

Templeton Hospital

Frequency, damping and modeshape estimates are presented in Table 2 and Figure 9. The first mode involves mostly transverse motion of the west wing, and the second mode is mostly north wing. Both wings contribute to the third mode. The instrumentation layout allows only the study of the north western wings of this very asymmetric building.

Table 2 contains result for the M 6.5 earthquake in 2003, three of its aftershocks and another smaller earthquake in 2005. Results seem to be consistent to the observations made from the analysis of the Parkfield school building. The amplitude dependence of the modal parameters is shown in Figures 10 and 11. Refer to Figure 4 for the acceleration time histories of the 2003 San Simeon earthquake.

Table 2. **Templeton hospital building frequency and damping estimates calculated from MODE-ID. The peak structural acceleration is provided for each earthquake**

Earthquake	Frequency (Hz) West Wing	Damping Ratio (%) West Wing	Frequency (Hz) East Wing	Damping Ratio (%) East Wing	Frequency (Hz) Mode 3	Damping Ratio (%) Mode 3
6.5 M 1.3 g 12/22/03	4.77	15.75	5.0	16.6	7.42	17.2
.031g 02/09/04 aftershock	7.09	21.1	7.4	11.6	10.7	16.0
.073g 05/02/04 aftershock	6.6	20.6	6.7	13.4	9.2	11.4
.217 g 10/02/04 aftershock	6.6	15.4	5.8	17.5	8.1	14.0
4.4 M .017 g 05/16/05	7.3	20.0	7.0	12.1	9.9	8.9

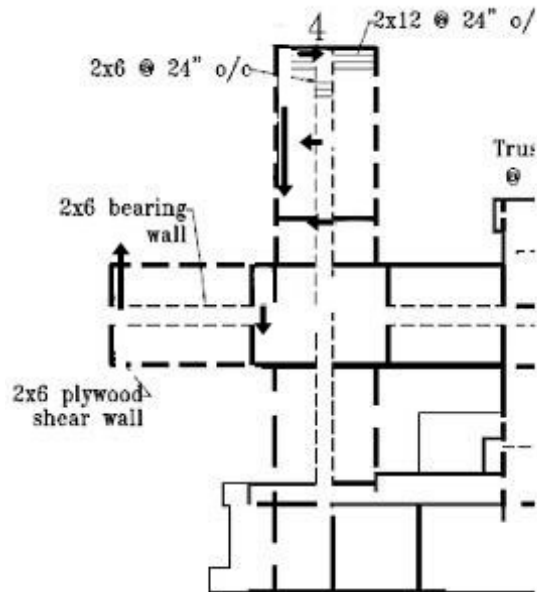**West Wing Mode**

North Wing Mode
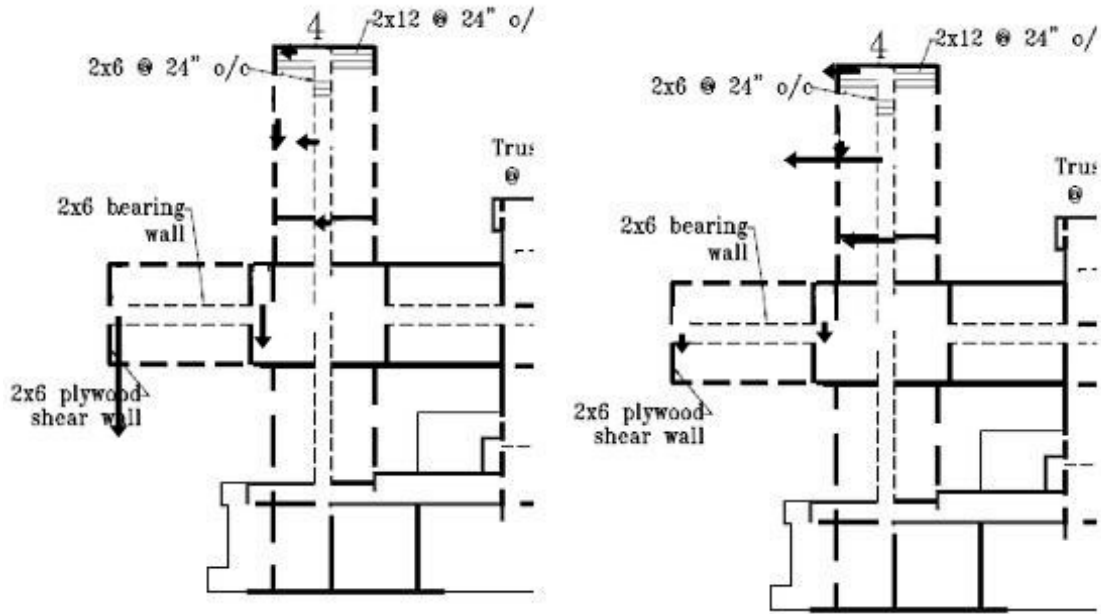
Mode 3

**Figure 9: First three modeshapes of the Templeton hospital building
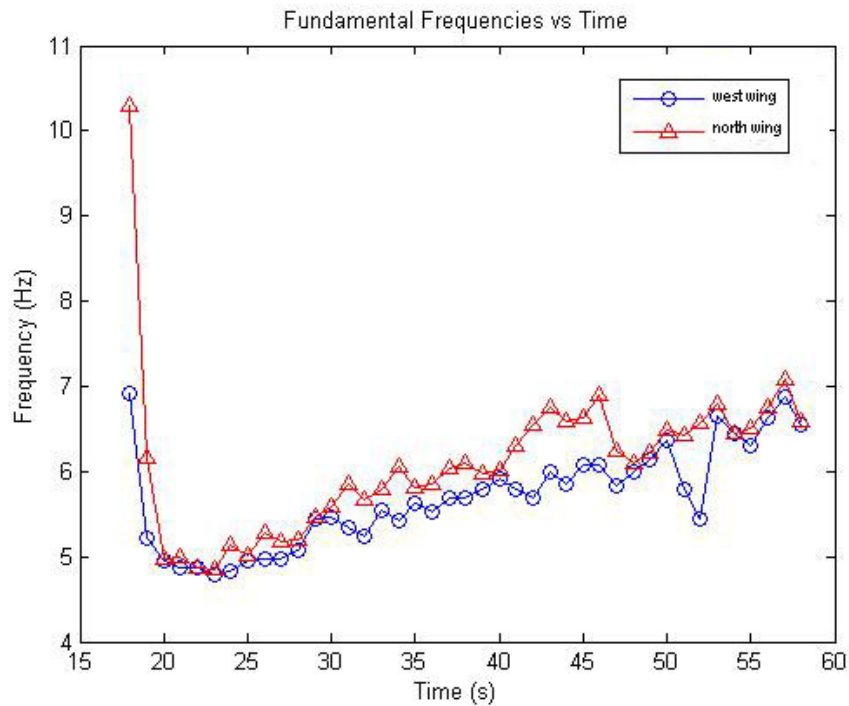generated from the 2003 San Simeon earthquake**

Figure 10: Amplitude dependence of the west wing and north wing frequency estimates for Templeton hospital building. The window analysis is performed on the 2003 San Simeon earthquake.
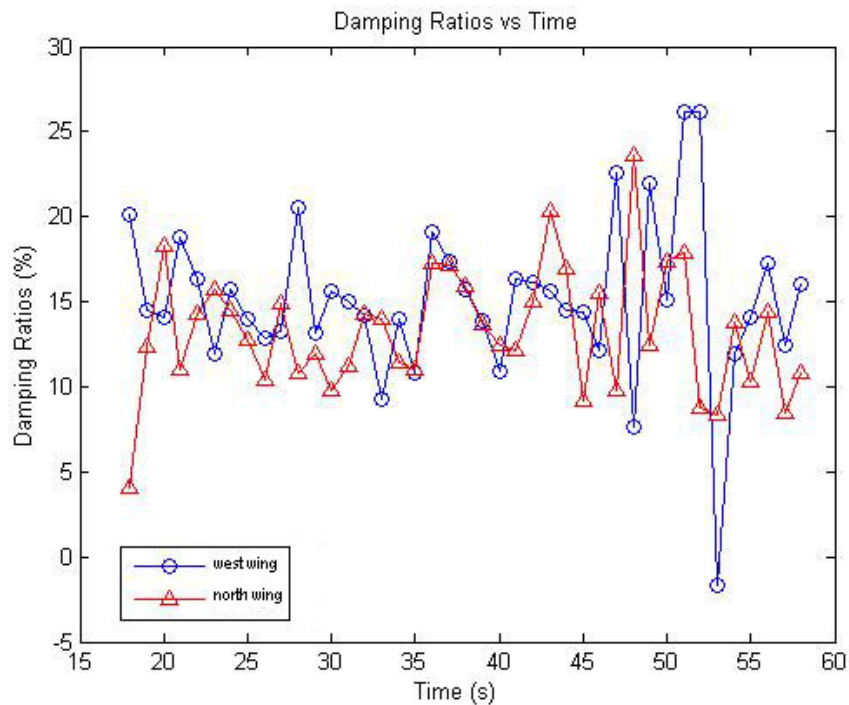

Figure 11: Amplitude dependence of the west wing and north wing mode damping estimates for Templeton hospital building. The window analysis is performed on the 2003 San Simeon earthquake.

Hysteresis Characterization

General Concepts

One of the major characteristic of wood-frame buildings is pinching hysteresis. As loading progresses and the deformation of the connection increases, wood fibers are crushed and a nail may begin to yield. If the loading is reversed, the nail moves through the gap formed by the crushed wood fibers. Through each cycle of displacement, depending on the amplitude of the motion, the wood is increasingly indented by the nail. This creates extra spacing wherein the nail will displace with reduced opposing force (Judd 2004).

It is imperative to accurately map hysteresis curves since they play a pivotal role in creating a better nonlinear model. Fortuantely, many of the commercial products that provide nonlinear analysis have the option to input a hysteresis model. The hysteretic behavior of a structure plays a crucial role in many current approaches to seismic performance-based analysis and design. Thus, many experiments have been performed to record hysteretic data for wood shear walls and other subassemblies. An example that illustrates the pinching behavior is show in Figure 2. Although thus test was for a single-nail connection, similar behavior is observed for wall and diaphragm components and for entire structures.
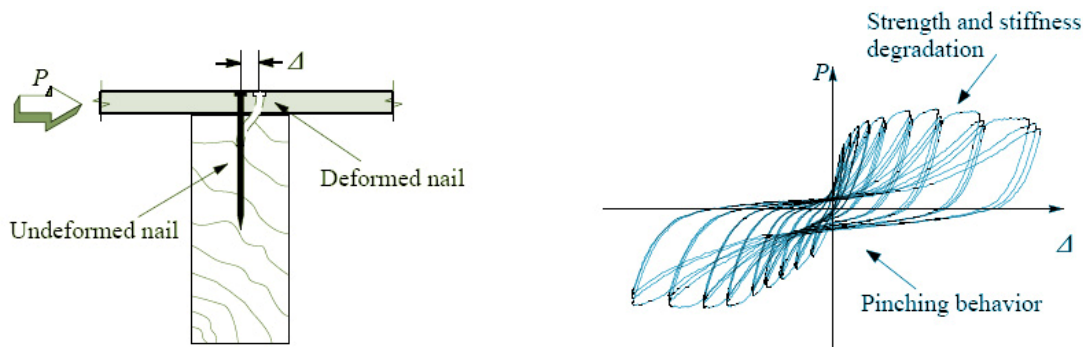

Figure 12. Illustration of the nailed sheathing connection and pinching hysteresis curve (Judd 2004).

Extraction of hysteretic characteristics of wood-frame building components can lead to an understanding of the pinching and degradation behavior as well as reveal the extent to which the building response extends into the nonlinear range. The process involves the construction of a hysteresis curve by plotting time history pairs of restoring force across the component (on the vertical axis) and relative displacement across the component (on the horizontal axis). The ability to compute the restoring force and relative displacement requires that sufficient instrumentation be present.
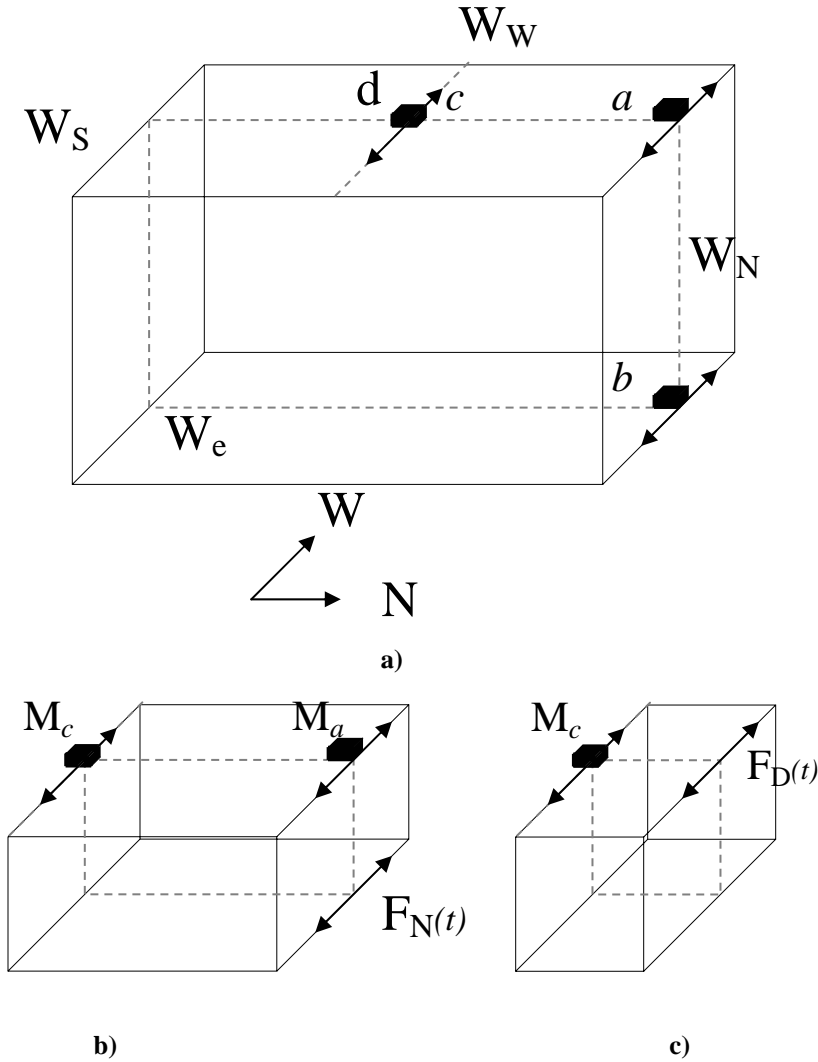
W_W

d c a

W_S

W_N

b

W_e

W

N

a)

M_c M_a M_c

$F_{D(t)}$

$F_{N(t)}$

b) **c)**

Figure 13: Illustrative example of the free body diagram concept to calculate a hystersis curve.

Consider the simple structure shown in Figure 13a as an example, consisting of north, south, east and west walls (W_N, W_S, W_E and W_W) and a diaphragm (D) with earthquake acceleration records obtained at *a*, *b* and *c* in the E-W direction. It is desired to plot the hysteretic curve for the north wall. To obtain the restoring (shear) force time history, a free-body diagram (FBD) is needed as shown in Figure 13b. The north wall is cut at mid-height and the diaphragm at mid-span as shown, with the cuts extending through the east and west walls. In the E-W direction, the restoring force at the diaphragm cut is set to zero based on an assumption of symmetric response, and the forces on the east and west walls are taken as zero because they would be out of plane, leaving only the restoring force F_N on the north wall. The E-W equation of motion is shown below in Equation 1

Equation 1. Force balance equation derived from FBD Figure 13b

$$F_N(t) = m_a \ddot{x}_a + m_c \ddot{x}_c$$

where m_a and m_c are tributary masses for the free body at a and c and $\ddot{x}_a$ and $\ddot{x}_c$ are the recorded accelerations at a and c, gives $F_N(t)$ directly. The relative displacement $x_{a\text{-}b}(t)$ across the north wall is obtained by subtracting the doubly integrated acceleration records at a and b. Pairs of $F_N(t)$ and $x_{a\text{-}b}(t)$ are then plotted.

The situation for the diaphragm is different because the shear varies substantially along the diaphragm, being maximum at the ends. The procedure employed here extracts the restoring (shear) force $F_D(t)$ at the quarter point and uses a free body consisting of one quarter of the diaphragm and adjacent pieces of the east and west walls cut at mid-height as shown in Figure 13c. With similar assumptions as made previously, only $F_D(t)$ is present and is determined from Equation 2

Equation 2: Force balance equation derived from FBD Figure 13 c

$$F_D(t) = m_c \ddot{x}_c$$

The relative displacement in this case is $x_{c\text{-}a}(t)$, obtained by subtracting the doubly integrated acceleration records at c and a.

Hysteresis Characteristics Results

Using the free body concept described in the previous section, attempts are made to retrieve the hysteretic characteristics of the Parkfield school and Templeton hospital buildings. Results for the Parkfield school are shown in Figure 14a (east wall), 14b (diaphragm), 15c (top part of south wall) and 15d (bottom part of south wall). For example, calculations performed for the hysteresis curve in Figure 14a are based on Equation 1, with the north wall in Figure 13 representing the east wall of the Parkfield school, and channels a, b and c in Figure 13 being channels 1, 3 and 2, respectively, at Parkfield school (see Figure 1). Since the ground motion is assumed to be uniform, it does not matter that channel 3 is not located directly under Parkfield school's east wall. For the masses m_c and m_a in Figure 13b, artificial values in the ratio of 1.3 to 1.0 are employed. The use of artificial values means that the force scale in Figure 14 is meaningless, but the shape of the hysteresis curve is not affected since this depends only on the ratio of m_c to m_a.

The computed hysteresis curve in Figure 14a shows evidence of pinching in the larger excursions, but not nearly as clear as that in Figure 12 obtained from a controlled laboratory experiment. Results for the south wall in Figure 14c and d can be described similarly. In the latter cases, some filtering of the displacement histories had to be done to remove long-period errors. The computed hysteresis curve for the diaphragm (Figure 14b) doesn't seem to have any realistic trends. The same can be said for the computed hysteresis curve for the north wall of the north wing of the Templeton hospital show in Figure 15, which also used the procedure described by Equation 1 and Figure 13.
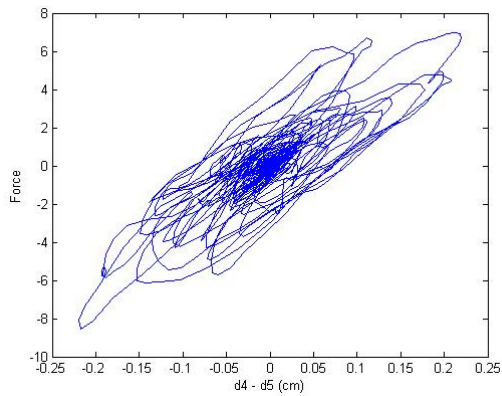
Hysteresis Curve of East Wall
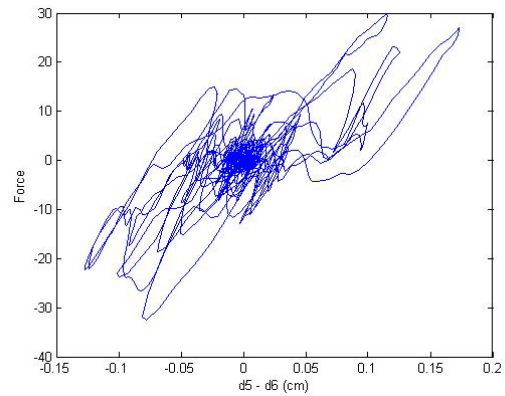

a)
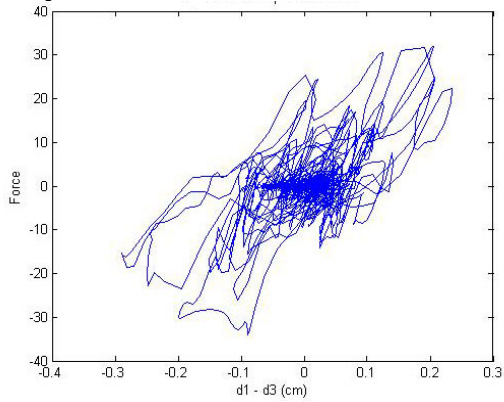
Hysteresis Curve of Diaphragm
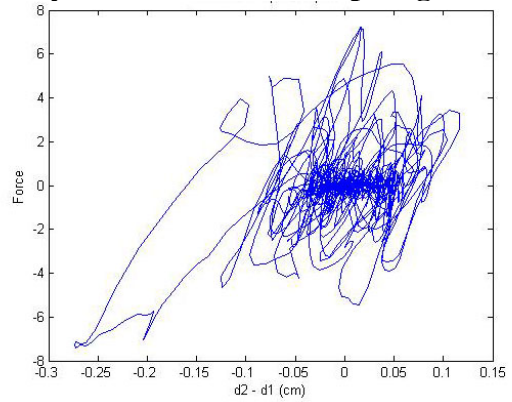
b)

Hysteresis Curve of Upper South Wall

c)

Hysteresis Curve of Lower South Wall

d)

Figure 14: Hysteresis curves of Parkfield school building

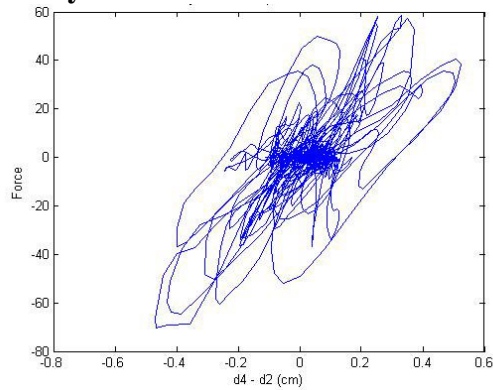## Hysteresis Curve of North Wall

Figure 15: Hysteresis curve of Templeton hospital building's north wall of its north wing

Conclusions

This study has observed significant amplitude dependence of the modal frequencies, decreasing for higher amplitude of shaking, and high damping values identified for the seismic response of wood-frame buildings. These results are in agreement with previous findings. A 25% to 30% drop in frequency during the stronger earthquakes examined here was typical. A damping ratio, more or less constant over the earthquake, at about 15% to 20% was also typical. A detailed study employing finite element models is planned to further investigate these behaviors.

An attempt to retrieve the hysteretic characteristics of wall and diaphragm components was hampered by errors inherent in the process employed. This process will also be a focus of the future finite element studies to determine what improvements in calculation process and instrumentation arrays can increase the accuracy of the computed hysteresis curves.

References

Beck JL. (1978). *Determining Models of Structures from Earthquake Records.* EERL Report No. 78-01, California Institute of Technology, Pasadena, Calif.

Beck JL. (1996) "System Identification Methods Applied to Measured Seismic Response," *Proceedings11th World Conference on Earthquake Engineering*, Acapulco, Mexico, June.

Beck RT., Beck JL. (1985). *Comparison Between Transfer Function and Modal Minimization Methods for System Identification.* EERL Report No. 85-06, California Institute of Technology, Pasadena, Calif.

Beck JL, Jennings PC. (1980). "Structural Identification Using Linear Models and Earthquake Records." *Earthquake Engineering and Structural Dynamics*, 8, 145-160.

Camelo V., Beck JL., Hall JF. (2002). "Dynamic Characteristics of Woodframe Structures." *CUREE Publication No. W-11*. CUREE Richmond, Calif.

Camelo VS, Beck JL, Hall JF. (2003). *Dynamic Characteristics of Woodframe Buildings*. Thesis, California Institute of Technology, Pasadena, Calif.

Ching J. Beck JL. Porter KA., Shaikhutdinov R. *Real-Time Bayesian State Estimation of Uncertain Dynamical Systems.* EERL Report No. 2004-01, California Institute of Technology, Pasadena, Calif.

Filiatrault A., et al. (2001). "Shake Table Tests of a Two-Story Woodframe House". *Element 1 Research Meeting, January 12, 2001*, CUREE-Caltech Woodframe Project, San Diego, Calif.

Foliente GC. (Ed.) (1994). "Analysis, Design and Testing of Timber Structures Under Seismic Loads." *Proceedings of a Research Workshop*, University of California, Forest Products Laboratory, Richmond, Calif.

Isoda H., Folz B., Filiatrault A. (2002). "Seismic Modeling of Index Woodframe Buildings." *CUREE Publication No. W-12*. CUREE Richmond, Calif.

Judd J., Fonseca F., (2004). Hysteresis Model Parameters for Nailed Sheathing Connections in Wood Shear Walls.

Mitrani J., Beck JL. (2003). User's Guide for MODE-ID Version 6.0. COMET website: http://comet.caltech.edu/sn_home.asp

Werner SD, Beck JL, Levine MB. (1987). "Seismic Response Evaluation of Meloland Road Overpass Using 1979 Imperial Valley Earthquake Records." *Earthquake Engineering and Structural Dynamics,* 15, 249-274.